# A non-filamentary model for unipolar switching transition metal oxide resistance random access memories

Kan-Hao Xue,[1,2,a] Carlos A. Paz de Araujo,[1,2] Jolanta Celinska,[2] and Christopher McWilliams[2]

[1]*Department of Electrical and Computer Engineering, University of Colorado, Colorado Springs, Colorado 80918, USA*
[2]*Symetrix Corporation, 5055 Mark Dabling Boulevard, Colorado Springs, Colorado 80918, USA*

A model for resistance random access memory (RRAM) is proposed. The RRAM under research utilizes certain transition metal oxide (TMO) such as NiO which shows unipolar switching behavior. The existence of metal/insulator states is not explained by filaments but attributed to different Hubbard $U$ values, which stems from an electron correlation effect. Current-voltage formulae are given both on the metal and insulator sides by putting the appropriate solutions of Hubbard model into the mesoscopic Meir-Wingreen transport equation. The RESET phenomenon is explained by a sufficient separation of Fermi levels in the electrodes and hence a Mott transition can be triggered in the anodic region due to a lack of electrons. The SET behavior originates from a tunneling current which removes the insulating region near the anode. Several experimental evidences are also presented to support this model. The model also serves as the theoretical prototype of Correlated Electron Random Access Memory (CeRAM) which is defined to be a TMO RRAM whose working mechanism is based on the strong electron correlation effects. © *2011 American Institute of Physics*. [doi:10.1063/1.3581193]

## I. INTRODUCTION

Resistance random access memory[1,2] (RRAM) is regarded as one of the most promising nonvolatile memories, especially for the high density memory market. Early RRAMs employed colossal magnetoresistive (CMR) thin films such as $Pr_{0.7}Ca_{0.3}MnO_3$ and $La_{0.7}Ca_{0.3}MnO_3$ as the resistance switching media, whose switching effects were reported by Asamitsu *et al.*,[3] Liu *et al.*,[4] etc. Nevertheless, CMR materials are poor in compatibility to the existing semiconductor technology since they consist of various metal elements and possess complicated structures. In recent years, certain transition metal binary oxides which also exhibit reliable resistance switching phenomena have attracted much attention.[5–8] Among these oxides, $Cu_xO$ and NiO take greater advantages because Cu and Ni themselves serve as interconnection materials in nanoscale semiconductor technology (Cu as widely used connecting wire and NiSi as interconnection material in 65 nm technology node and beyond[9]) such that element contamination is eliminated. Baek *et al.* showed that RRAM made of NiO had the lowest operation current.[5] Besides, NiO exhibits stable unipolar (symmetric) switching properties, as confirmed by many groups.[7,10] Considering all aspects, NiO is an excellent candidate for RRAM applications presently.

Various theories and models have been proposed to explain the resistance switching mechanisms in RRAMs, including filamentary conduction model,[8,10] space-charge-limited conduction model,[6] domain tunneling model with Mott transition,[11,12] etc. Nevertheless, we should be aware that different types of RRAM may originate from totally dif-ferent mechanisms. There is no common understanding in RRAM's intrinsic bi-stable resistive states from a physics point of view. In this paper, however, we shall focus on the unipolar switching phenomenon, exemplified by NiO. Practically, unipolar switching has advantages over bipolar switching because no negative voltage pulses are needed.

The prevailing model for NiO RRAM is the filament model.[8] This model states that NiO thin films are insulators as they are deposited. A high voltage pulse is then applied through the thin film and filaments emerge in this "electroforming" process. After forming, NiO becomes a metal through those conducting filaments. When the applied voltage reaches a certain $V_{RESET}$, the filaments will be ruptured by the Joule heating caused by strong current and hence NiO becomes an insulator again. However, there exists another threshold voltage $V_{SET}$, which is higher than $V_{RESET}$ but lower than the electroforming voltage ($V_{FORM}$), where conducting filaments will re-emerge and NiO turns to a metal again. The two stable resistance states are switched by rupture and reformation of conducting filaments.

The electroforming process is necessary for the validity of filament model. Nevertheless, our previous works on NiO RRAM (Refs. 13–15) reveal that NiO can be fabricated to be a metal in its virgin state (achieved by doping with extrinsic nickel carbonyl ligands) and no electroforming step is needed (shown in Fig. 1). Such NiO thin films exhibit reliable bi-stable resistance states and are very suitable for RRAM application. In the absence of electroforming, a new model is needed for theoretical description. Furthermore, the filament model ascribes the rupture of filaments to Joule heating, which depends on the power through the device. In our NiO thin films, the product of voltage and current can usually be higher at the SET point compared with the
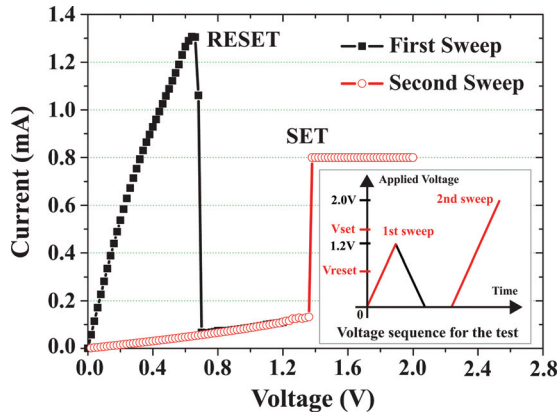
a)Electronic mail: xuekanhao@gmail.com.

FIG. 1. (Color online) The I-V characteristic of an RRAM without electro-forming (CeRAM).

RESET point (see Fig. 1). If the current compliance (i.e., the external limit on current) is high, we may even have $I_{SET} > I_{RESET}$.[15] A difficulty then arises as to why the filaments are not ruptured immediately following the SET operation. In the present study, we shall propose a nonfilamentary model according to the Mott-Hubbard picture for such NiO RRAMs.

## II. A MODEL BASED ON MOTT-HUBBARD PICTURE

### A. The two resistance states

Transition metal cations, typically for those $3d$ transition metals, often involve certain $d$ electrons that do not participate in ionic bonding. The status of $3d$ electrons is between the localized states (like $4f$ electrons in lanthanides) and delocalized Bloch states (like $4s$ electrons). Band theory itself is insufficient to describe the behaviors of those electrons. In 1937, NiO was first proposed to be a counter-example of band theory by de Boer and Verwey.[16] The electron configuration of $Ni^{2+}$ is $1s^2 2s^2 2p^6 3s^2 3p^6 3d^8$. Since NiO possesses the rock salt structure, the $3d$ band of $Ni^{2+}$ will be split by the octahedral ligand field to give $e_g$ and $t_{2g}$ subbands (shown in Fig. 2). There is no degeneracy for high spin and low spin states in $3d^8$, because both of them give $e_g^2 t_{2g}^6$. It is then obvious that the $e_g$ subband is half-filled, because it can accommodate 4 electrons in total. According to band theory,[17] NiO should be a metal, though it is well known that NiO is an insulator with bandgap $E_g \simeq 4.3$ eV.[18] The discrepancy has been attributed to the electron correlation effects, since two opposite-spin electrons sharing the same $3d$ orbital would experience strong Coulomb repulsion force
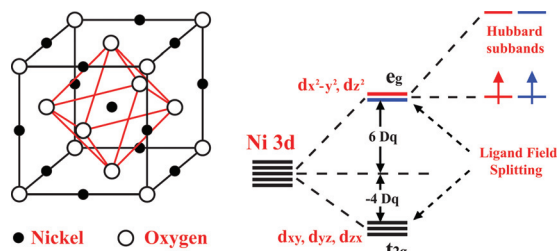


FIG. 2. (Color online) The crystal structure and band diagram for NiO.
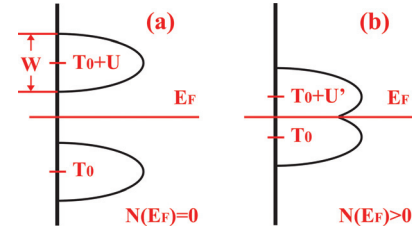


FIG. 3. (Color online) Density of states for NiO: (a) the normal case, insulator; (b) metallic NiO. $W$ is the bandwidth.

with each other. The extra energy cost for two electrons to share the same $3d$ orbital is called the "Hubbard $U$":

$$U = \int d\vec{r}_1 \int d\vec{r}_2 |\phi(\vec{r}_1)|^2 \frac{e^2}{4\pi\varepsilon|\vec{r}_1 - \vec{r}_2|} |\phi(\vec{r}_2)|^2, \qquad (1)$$

where $\varepsilon$ is the permittivity[19] and $\phi$ represents atomic wave functions.

The insulating nature of NiO is strongly related to this Hubbard $U$. Nevertheless, if for some reason the value of $U$ decreases below a certain threshold, NiO is contrarily expected to be a metal, as the band theory states. Such a transition does not seem practical for bulk NiO at room temperature and atmospheric pressure, but for thin films this possibility cannot be ruled out. The screening effect, indeed, may reduce the Hubbard $U$. In Eq. (1), the permittivity accounts for the screening. In the limiting case, a perfect metal will have divergent permittivity, which means $U$ becomes negligible. In thin films, extra electrons can tunnel into the material and high electron concentration would induce a strong screening effect that tends to diminish the Hubbard $U$.

Figure 3 illustrates the density of states (DOS) for the two cases of metallic/insulating NiO. The criterion for identifying a metal or insulator is whether there is a nonzero DOS at the Fermi level. The Hubbard $U$ is altered by electron concentration. This is a self-containing argument since once NiO becomes a metal, the screening is strong and $U$ is reduced. Otherwise, $U$ is huge and NiO remains an insulator with poor screening.

Another viewpoint on this is the Mott criterion,[20–22] which states that the material is a metal if:

$$n^{1/3} a_B > 0.26, \qquad (2)$$

where $n$ is the free electron concentration and $a_B = 4\pi\varepsilon\hbar^2 / me^2$ is the effective Bohr radius. The experimental finding is that NiO thin film (doped with carbonyl) can be fabricated to be a metal and hence Eq. (2) is satisfied in the virgin state,[14] though such situation cannot be satisfied in the bulk. A decrease in the electron concentration, however, may lead to $n^{1/3} a_B < 0.26$ and a metal-to-insulator Mott transition then occurs.

### B. Transport equation and the model Hamiltonian

To model the transport in such NiO thin films, it is desirable to notice that the film thickness of such NiO is about 60 nm, which is usually in the mesoscopic transport regime. In addition, electron correlation effects should also be taken

into account. Meir and Wingreen[23] proposed a quantum transport formula in 1992 to incorporate electron correlation:[24]

$$I = \frac{2\pi i q}{h^2} \int dE [f_L(E) - f_R(E)] \, Tr[\Gamma(G^r - G^a)],$$
$$(q = -e = -1.602 \times 10^{-19} \, C). \quad (3)$$

where $f_{L,R}(E)$ are Fermi-Dirac distribution functions in the two leads; $\Gamma \equiv \Gamma_L \Gamma_R / (\Gamma_L + \Gamma_R)$ is a coupling parameter for NiO and the leads; $G^r$, $G^a$ are the retarded and advanced Green's functions that involve electron correlation. This serves as a convenient way to solve the problem.

The Green's functions $G^r$, $G^a$ come from the model Hamiltonian. We here use the notable Hubbard model[25] and wish to recover the qualitative, rough picture of the DOS in Sec. II A. To discuss narrowband electrons with strong correlation, the Wannier representation would be a better choice.

$$H = \sum_{i,j} \sum_{\sigma} T_{ij} c_{i\sigma}^{\dagger} c_{j\sigma} + \frac{U}{2} \sum_i \sum_{\sigma} \hat{n}_{i,\sigma} \hat{n}_{i,-\sigma}, \quad (4)$$

where $c_{i\sigma}^{\dagger}$ and $c_{j\sigma}$ are electron creation and annihilation operators in Wannier representation; $T_{ij}$ represents hopping integral between site $i$ and site $j$; $\hat{n}_{i,\sigma} = c_{i\sigma}^{\dagger} c_{i\sigma}$ is the occupation number operator for site $i$ with spin $\sigma$. To solve the retarded/advanced Green's functions for this Hamiltonian, an equation of motion method introduced by Zubarev[26] is convenient. The Hubbard model is not exactly solvable in general, yet an infinitely narrowband approximation would give exact solutions.

$$T_{ij} \rightarrow T_0 \delta_{ij} \quad (5)$$

$$H = T_0 \sum_i \sum_{\sigma} \hat{n}_{i,\sigma} + \frac{U}{2} \sum_{i,\sigma} \hat{n}_{i,\sigma} \hat{n}_{i,-\sigma} \quad (6)$$

Hubbard himself solved his model in the infinitely-narrowband limit. The trick is for fermions, $n^2 = n$ always holds regardless of which value (0 or 1) $n$ is. The results are:

$$G_{ij\sigma}^{r,a}(E) = \hbar \delta_{ij} \left[ \frac{1 - \langle \hat{n}_{-\sigma} \rangle}{E - T_0 \pm i0^+} + \frac{\langle \hat{n}_{-\sigma} \rangle}{E - (T_0 + U) \pm i0^+} \right], \quad (7)$$

$$Tr(G^r - G^a) = 2\pi i N \hbar [(1 - \langle \hat{n}_{-\sigma} \rangle) \, \delta(E - T_0) + \langle \hat{n}_{-\sigma} \rangle$$
$$\times \delta(E - T_0 - U)], \quad (8)$$

where $N$ is the number of sites and the average occupation of -$\sigma$ spin states is $\langle \hat{n}_{-\sigma} \rangle = 1/2$ for NiO, in both antiferromagnetic and paramagnetic (above Néel point) phases.

The infinitely-narrowband approximation is acceptable for the insulator side, but not for the metal side because $3d$ electrons can hop to other sites in a metallic NiO. We are content with the DOS of two delta-functions for the insulator side, yet to go to the metal side that approximation must be exceeded. Hence, no exact solution of Hubbard model is available for the metal side and RESET. As far as a first order model is concerned, we may still rely on the results (7) and (8), but allow two modifications: (1) the Hubbard $U$

being smaller; (2) finite band-width effects. Instead of solving the Hubbard model in this case, we use a plausible assumption on the DOS: it has a Lorentzian-form shape. $N(E) \sim Tr(G^r - G^a)$

$$= iN\hbar \left\{ \frac{b}{(E - T_0)^2 + b^2} + \frac{b}{[E - (T_0 + U')]^2 + b^2} \right\}, \quad (9)$$

where this metallic $U'$ is smaller than the insulator case. The parameter $b$ is the half width at half maximum for the Cauchy-Lorentz distribution.

The next step is to derive the I-V relationship both on the metal side and on the insulator side, which is carried out in the following sections.

## C. Modeling of the metal side and RESET

Starting from the metal side, we shall put the solution of the Hubbard model (9) into the Meir-Wingreen formula (3). Reset the energy zero point to $(T_0 + U'/2)$ for convenience and by symmetry the electrochemical potentials in both electrodes are simply:

$$\mu_L = -\frac{eV}{2}; \quad \mu_R = \frac{eV}{2}. \quad (10)$$

Another assumption here is also based on the symmetry of the device:

$$\Gamma_L = \Gamma_R = \gamma; \quad \Gamma \equiv \frac{\Gamma_L \Gamma_R}{\Gamma_L + \Gamma_R} = \frac{\gamma}{2}. \quad (11)$$

The parameter $\gamma$ has the unit of energy and $\gamma/\hbar$ can be explained as an "escape rate" from the leads.[27] It clearly reflects the coupling between the leads and the NiO sample. Subsequently we obtain:

$$I = \frac{qN\gamma}{2h} \int dE \left\{ \frac{1}{exp[(E + eV/2)/kT] + 1} \right.$$
$$\left. - \frac{1}{exp[(E - eV/2)/kT] + 1} \right\}$$
$$\times \left[ \frac{b}{(E + U'/2)^2 + b^2} + \frac{b}{(E - U'/2)^2 + b^2} \right]. \quad (12)$$

To plot the I-V curve for the metal side, two parameters are still missing: (1) the metallic $U'$; (2) the parameter $b$. For reasons that will be clear later, a possible choice of choosing $U'$ and $b$ is:

$$U' = 2b = \frac{eV_{SET}}{2}. \quad (13)$$

A nonzero $U'$ then implies a "correlated metal." Another choice, with even more drastic approximation, is to choose $U' = 0$ (normal metal) while keeping $b$ unchanged. Given $V_{SET} = 1.4 \, V$, the two simulation results for the I-V on the metal side at $T = 300 \, K$ are shown in Fig. 4.

The simulation results do not reveal a RESET phenomenon, nor even a negative differential resistance (NDR). The NDR phenomenon has been widely found in, for example, Esaki diode and GaAs MESFET. Nevertheless, NDR does
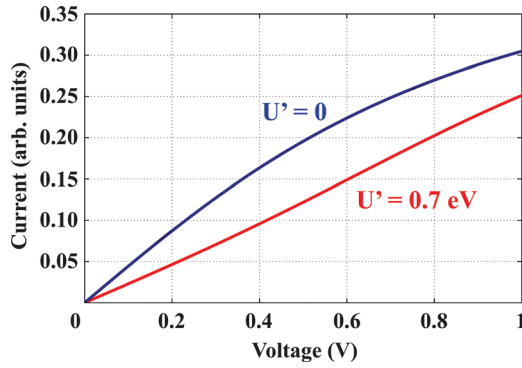
FIG. 4. (Color online) Simulation results of the I-V curve on the metal side. Given $V_{SET} = 1.4$V.

not imply a memory transition to the insulator side. The fact of RESET in TMO RRAMs seems peculiar at first glance since it is an increased applied voltage rather than a decreased voltage that renders a transition from a metal to an insulator. It has been argued in Sec. II A that a diminished electron concentration may indeed trigger such a transition. Yet, Kirchhoff's law simply states that the total electron number inside NiO could not vary even if a voltage is applied. This, however, does not preclude a local electron concentration variation inside NiO when it comes to a none-quilibrium problem. The average quasi-Fermi level through the device is sketched in Fig. 5.[28] We assume transport inside NiO is ballistic and the voltage drop occurs near the two leads. If there exist scattering centers inside NiO, extra voltage drops will occur there as well, but this does not affect our understanding. As the figure demonstrates, the lead area near the anode (named Region-1) suffers from an electron deficit while the lead area near the cathode accommodates extra electrons injected from the cathode. The deficit/excess

of electrons can also be understood when considering the procedure of establishing a stable current. Electrons near the anode are extracted out while electrons from the cathode enter the lead adjacent to it, causing net electron concentration variations in Region-1 and Region-3 until the current is stable under a certain applied voltage. The higher the applied voltage, the more severe the electron deficit occurs in Region-1. Before $V_{RESET}$, such deficit is not enough to cause a Mott transition. A RESET voltage then corresponds to a critical Mott electron concentration $n_c$ [determined by Eq. (14)] in Region-1 and as Region-1 becomes insulating, the total current drops sharply.

$$n_c^{1/3} a_B = 0.26. \tag{14}$$

The present model predicts that the metal-to-insulator transition only occurs in the anodic region, which is exactly confirmed by the transmission electron microscopy (TEM) results from Park *et al.*[29] They have discovered that in NiO RRAM, only the anodic (rather than cathodic) region changes during SET and RESET. In addition, the polarity-dependent sputtering damage experiment by Kinoshita *et al.*[30] also lends strong support to this.

To include the RESET mechanism into Eq. (12), we may multiply it by a Heaviside step function $\Theta(V_{RESET} - V)$.

### D. Modeling of the insulator side and SET

After RESET, Region-1 becomes insulating while the rest of NiO is still metallic. In the derivations below, we treat the metallic NiO together with the cathode as a single electrode. Only Region-1 will be regarded as the "insulator" to be studied. Now starting from the insulator side, we put the solution of the Hubbard model (8) into the Meir-Wingreen formula (3) and obtain:

$$I = \frac{\pi q N \gamma}{2h} \left\{ \frac{1}{\exp[(eV - U)/2kT] + 1} - \frac{1}{\exp[-(eV + U)/2kT] + 1} + \frac{1}{\exp[(U + eV)/2kT] + 1} - \frac{1}{\exp[(U - eV)/2kT] + 1} \right\}. \tag{15}$$

The parameter $U$ in this equation is simply related to the SET voltage:

$$U = eV_{SET}, \tag{16}$$

since mathematically, the point $eV = U$ is the turning point of the current at zero absolute temperature.

At a testing $V_{SET}$ of 1.4 V, the I-V curve calculated from this model is demonstrated in Fig. 6 ($T = 300$ K). A sharp current increase occurs around $V_{SET}$, which originates from a quantum tunneling effect. The simulation result reveals a saturating current, which is not correct. In this model we have assumed NiO to be a Mott insulator. Nevertheless, the lower Hubbard subband of nickel makes strong hybrid orbitals with the oxygen 2$p$ band.[18] Furthermore, there is already a common understanding that NiO is a "charge transfer insulator"[31] rather than "Mott insulator." The available DOS is sufficient even if the applied voltage reaches $V_{SET}$. Notwithstanding this discrepancy, the approximation of using Mott
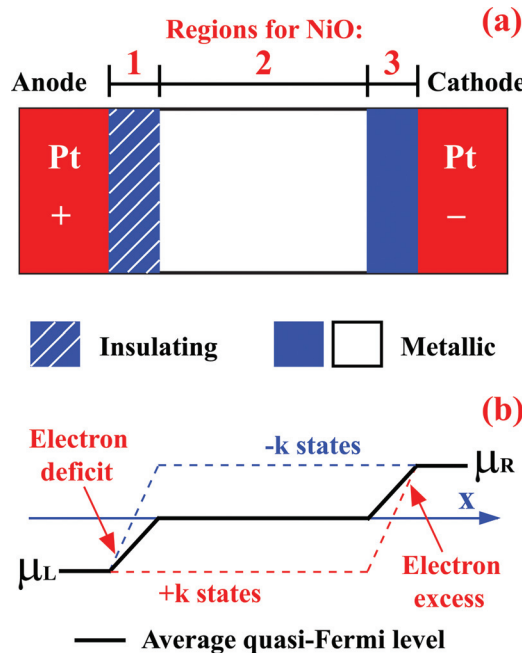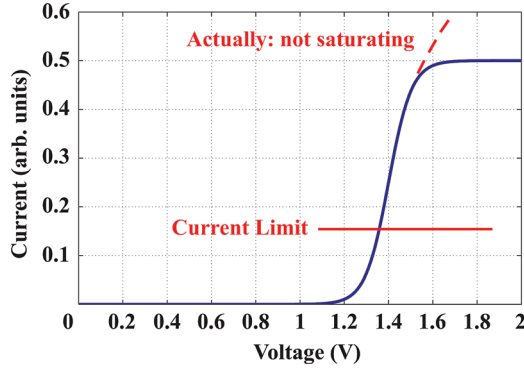


FIG. 5. (Color online) (a) Device structure and three regions in NiO; (b) quasi-Fermi levels through the device at the RESET point, bold line for the average quasi-Fermi level.

FIG. 6. (Color online) Simulation result of the I-V curve on the insulator side. Given $V_{SET} = 1.4$V.



FIG. 7. (Color online) Graphic estimation of $V_{RESET}$.

insulator does not in fact influence our qualitative understanding of NiO RRAM.

As this model shows, a high tunneling current emerges when $V$ reaches $V_{SET}$. This current, if not constrained by external circuits, would cause permanent damage to the NiO thin films. Thus, a current limit must be set in order to protect the device. There is, however, an important issue here whether NiO in Region-1 would become a metal after this current. So far as the current limit is not too low, an insulator-to-metal transition indeed occurs.[15] It is crucial to separate the voltage and the current when it comes to SET. The voltage merely serves as a trigger mechanism which accounts for the tunneling. The high current is the real mechanism for memory switching in that it compensates the electron deficit and recovers the electron concentration in Region-1.

### E. Further discussions and experimental support

The validity of Eq. (13) can now be examined. In Sec. II D, $eV_{SET}$ has been set equal to the insulating effective Hubbard $U$. To ensure there is no DOS at the Fermi level on the insulator side, $2b < U$ must be satisfied. A fairly reasonable choice is to let $b = U/4$. On the other hand, the metallic $U'$ cannot be too large because the tested I-V curves are never convex functions. Simulation results show that $U' = 2b = U/2$ gives a linear function while $U' = 0$ gives a concave function. We choose $U' = 2b = U/2$ for a linear I-V shape. Both of these choices are intrinsically arbitrary since the exact solution of Hubbard model is not known.

Figure 7 illustrates a graphic method to estimate $V_{RESET}$ in terms of $V_{SET}$ under the approximation of Eq. (13). Assume RESET corresponds to a Fermi level splitting such that the metallic "upper Hubbard subband" becomes empty in Region-1. The probability density function of a Cauchy-Lorentz distribution becomes negligible if deviation from the center is more than $2b$. Hence, rough estimation gives:

$$\frac{eV_{RESET}}{2} = 2b - \frac{U'}{2} = \frac{U}{4} = \frac{eV_{SET}}{4} \Rightarrow V_{RESET} = \frac{V_{SET}}{2},$$
(17)

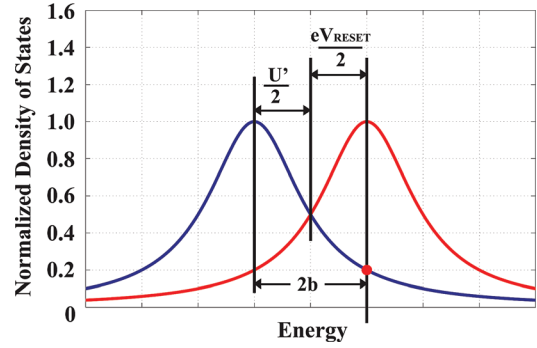which fits the experimental results (as an example, see Fig. 1) qualitatively.

It is now possible to address several other experimental results within the framework of this model.

(1) $V_{RESET}$ is more stable than $V_{SET}$.

According to the model, every time starting from a metal, the sample is almost the same even in Region-1, since the insulating region has already been removed. However, every time RESET happens, the thickness and shape of Region-1 may vary. Starting from a variable insulator, the SET voltage is prone to dispersion. This is consistent with our experimental results.[15]

(2) RESET depends much more on the voltage than the current.

Among various tests on the RESET, the current $I_{RESET}$ could vary substantially (due to SET compliance or doping conditions), yet $V_{RESET}$ exhibits very little dispersion.[15] The RESET phenomenon neither depends on the current, nor on the resistance or power, but rather on a critical $V_{RESET}$. This can be well explained in the present model since the metal-to-insulator transition in Region-1 is caused by a separation of Fermi levels which is due to the applied voltage. Current does not play a direct role in this mechanism. This is in contrast to the SET phenomenon, where a high tunneling current accounts for the memory switching and voltage merely serves as a trigger mechanism for the current.

(3) In RRAMs that require electroforming, $V_{FORM}$ is generally much larger than $V_{SET}$. In addition, $V_{FORM}$ is film thickness dependent; $V_{SET}$ is not.

This is well explained according to the present model. If NiO (or equivalent TMO materials) is fabricated to be an insulator in its virgin state, we must pass a high current through the entire thickness of the NiO sample (60 nm, for example), rather than only the anodic Region-1, which is much thinner such that tunneling occurs easily. On the other hand, if NiO is fabricated to be a metal, film break down never occurs and the only possible insulating region is the small anodic volume of Region-1. Our model further predicts that $V_{FORM}$ is proportional to the film thickness, while $V_{SET}$ does not have such dependence because it is only susceptible to the thickness and shape of Region-1. Direct experimental support comes from Baek *et al.*,[5] who reported that in NiO $V_{FORM}$ is almost linearly dependent on film thickness, but $V_{SET}$ is not. It is due to such difference that they proposed a method of

under-oxidation to reduce $V_{FORM}$ to the same level of $V_{SET}$.

## III. THE CONCEPT OF CORRELATED ELECTRON RANDOM ACCESS MEMORY (CERAM)

The switching mechanisms in the present model are based on an electro-induced Mott (or, "charge transfer") transition. Particularly, the TMO thin films are fabricated to be metallic as-deposited such that no electroforming is needed. Although an electroformed TMO thin film may still exhibit similar I-V characteristics, the electroforming procedure generally incurred defects or structure damages. Defects in the thin films may also cause resistance switching by trapping and de-trapping effects. After all, metal-insulator transition is a very complicated phenomenon and various mechanisms could exist. The working mechanism of a practical TMO RRAM device may be in one of the three cases: (1) electron correlation; (2) trapping and de-trapping by defects; (3) a mixture of both. Considering RRAM is a much general definition, we would like to introduce here the particular definition of Correlated Electron Random Access Memory (CeRAM): a TMO-based RRAM whose resistance switching is caused by strong electron correlation effects. CeRAM starts as a metal rather than an insulator. The definition of CeRAM excludes the possibility of defect-induced transition. The reliability of CeRAM (e.g., the thermal stability of the low resistance state)[14] is high because of its intrinsic physics as described above.

## IV. CONCLUSION

In summary, we have proposed a first order model of unipolar switching TMO RRAM based on the Mott-Hubbard picture. The insulator side corresponds to a Mott insulator or a charge transfer insulator whose insulating nature is caused by a large Hubbard $U$ coming from electron correlation effects. The metal side corresponds to a high electron concentration case, where strong screening has diminished this Hubbard $U$. Theoretical I-V formulae of both sides are obtained by incorporating the approximate solutions of the Hubbard model into the Meir-Wingreen formula. The transition from a metal to an insulator (RESET) is explained by a sufficient separation of Fermi levels in the leads. The anodic region suffers from an electron deficit and hence a Mott transition is triggered. The transition from an insulator to a metal (SET) is due to quantum tunneling effects triggered by a high voltage. The tunneling current removes the insulating region near the anode by strong screening. This model successfully explains several experimental facts such as: (1) only anodic region in NiO varies during SET and RESET under TEM inspection; (2) the higher stability of $V_{RESET}$ compared with $V_{SET}$; (3) the large current dispersion at RESET; (4) in NiO RRAMs that require electroforming, $V_{FORM}$ is proportional to film thickness while $V_{SET}$ is not. Finally, we have proposed a concept of Correlated Electron Random Access Memory (CeRAM): a TMO-based RRAM

whose working mechanism originates from the strong electron correlation effects as stated in the current paper.

[1] W. W. Zhuang, W. Pan, B. D. Ulrich, J. J. Lee, L. Stecker, A. Burmaster, D. R. Evans, S. T. Hsu, M. Tajiri, A. Shimaoka, K. Inoue, T. Naka, N. Awaya, K. Sakiyama, Y. Wang, S. Q. Liu, N. J. Wu, and A. Ignatiev, in *IEDM Technical Digest*, San Francisco, December 8-11, 2002, IEEE p. 193.
[2] R. Waser and M. Aono, Nat. Mater. **6**, 833 (2007).
[3] A. Asamitsu, Y. Tomioka, H. Kuwahara, and Y. Tokura, Nature **388**, 50 (1997).
[4] S. Q. Liu, N. J. Wu, and A. Ignatiev, Appl. Phys. Lett. **76**, 2749 (2000).
[5] I. G. Baek, M. S. Lee, S. Seo, M. J. Lee, D. H. Seo, D.-S. Suh, J. C. Park, S. O. Park, H. S. Kim, I. K. Yoo, U. Chung, and J. T. Moon, in *IEDM Technical Digest*, San Francisco, December 13-15, 2004, IEEE p. 587.
[6] A. Chen, S. Haddad, Y. C. Wu, Z. Lan, T. N. Fang, and S. Kaza, Appl. Phys. Lett. **91**, 123517 (2007).
[7] D. Ielmini, C. Cagli, and F. Nardi, Appl. Phys. Lett. **94**, 063511 (2009).
[8] U. Russo, C. Cagli, and A. L. Lacaita, IEEE T. Electron Dev. **56**, 186 (2009).
[9] International Technology Roadmap for Semiconductors (ITRS) 2007. Available at http://www.itrs.net/Links/2007ITRS/2007_Chapters/2007_Interconnect.pdf.
[10] D. C. Kim, S. Seo, S. E. Ahn, D.-S. Suh, M. J. Lee, B.-H. Park, I. K. Yoo, I. G. Baek, H.-J. Kim, E. K. Yim, J. E. Lee, S. O. Park, H. S. Kim, U. Chung, J. T. Moon, and B. I. Ryu, Appl. Phys. Lett. **88**, 202102 (2006).
[11] M. J. Rozenberg, I. H. Inoue, and M. J. Sánchez, Phys. Rev. Lett. **92**, 178302 (2004).
[12] M. J. Sánchez, M. J. Rozenberg, and I. H. Inoue, Appl. Phys. Lett. **91**, 252101 (2007).
[13] J. Celinska, M. D. Brubaker and C. A. Paz de Araujo, U.S. Patent No. 7,639,523 B2 (2009).
[14] J. Celinska, C. McWilliams, C. A. Paz de Araujo, and K.-H. Xue, "Material and Process Optimization of Correlated Electron Random Access Memories (CeRAMs)," J. Appl. Phys. (in press).
[15] C. McWilliams, J. Celinska, C. A. Paz de Araujo and K.-H. Xue, "Device Characterization of Correlated Electron Random Access Memories (CeRAMs)," J. Appl. Phys. (in press).
[16] J. H. de Boer and E. J. W. Verwey, Proc. Phys. Soc. **49**, 59 (1937).
[17] A. H. Wilson, Proc. R. Soc. A **133**, 458 (1931).
[18] G. A. Sawatzky and J. W. Allen, Phys. Rev. Lett. **53**, 2339 (1984).
[19] Here we use an effective permittivity $\varepsilon$ rather than the vacuum permittivity $\varepsilon_0$ in order to incorporate screening effects. A similar argument can be found in the footnote of N. F. Mott, *Metal-Insulator Transitions*, 2nd Ed. (Taylor and Francis, London, 1990), p. 80.
[20] N. F. Mott, Rev. Mod. Phys. **40**, 677 (1968).
[21] P. P. Edwards and M. J. Sienko, Phys. Rev. B **17**, 2575 (1978).
[22] N. F. Mott, *Metal-Insulator Transitions*, 2nd Ed. (Taylor and Francis, London, 1990), p. 128.
[23] Y. Meir and N. S. Wingreen, Phys. Rev. Lett. **68**, 2512 (1992).
[24] The present formula differs from Meir and Wingreen's result by a coefficient $1/\hbar$. This is because in their original work, the Dyson equations in the Keldysh formalism originated from the form $G = G_0 + G_0 \Sigma G$, where the $1/\hbar$ coefficient on the last term was set to 1.
[25] J. Hubbard, Proc. R. Soc. A **276**, 238 (1963).
[26] D. N. Zubarev, Usp. Fiz. Nauk. **71**, 71 (1960) [Sov. Phys. Usp. **3**, 320 (1960)].
[27] S. Datta, *Quantum Transport: Atom to Transistor* (Cambridge University Press, Cambridge, 2005), pp. 8–9.
[28] For an explanation of Fig. 5(b), see S. Datta, *Electronic Transport in Mesoscopic Systems* (Cambridge University Press, Cambridge, 1995), pp. 55–57, 65–66.
[29] G.-S. Park, X.-S. Li, D.-C. Kim, R.-J. Jung, M.-J. Lee, and S. Seo, Appl. Phys. Lett. **91**, 222103 (2007).
[30] K. Kinoshita, T. Tamura, M. Aoki, Y. Sugiyama, and H. Tanaka, Appl. Phys. Lett. **89**, 103509 (2006).
[31] J. Zaanen, G. A. Sawatzky, and J. W. Allen, Phys. Rev. Lett. **55**, 418 (1985).